Received 28 May 2006
Revised 27 December 2006
Accepted 21 February 2007

# Numerical solution of three-dimensional viscous shock layer using axisymmetric analog along the streamlines

S. Noori, S.M.H. Karimian and M. Malekzadeh Dirin
*Aerospace Engineering Department, Amirkabir University of Technology, Tehran, Iran*

## Abstract

**Purpose** – This paper aims to predict aerodynamic heating through the efficient solution of three-dimensional viscous shock layer (VSL) equations, using axisymmetric analog.

**Design/methodology/approach** – The three-dimensional VSL equations are written in the curvilinear streamline coordinate system. In these equations, normal momentum equation is replaced by Maslen's pressure relation. In addition to this, axisymmetric analog is implemented along the streamlines through assuming a zero value for circumferential velocity component. In this case, three-dimensional VSL equations are reduced into an axisymmetric form, which can be solved much easier.

**Findings** – It is demonstrated that the solution of three-dimensional VSL equations in the curvilinear streamline coordinate system, using axisymmetric analog, has made it possible to predict convective heat fluxes in both windward and leeward regions. Moreover, in comparison with the 3D VSL methods, the present approach dramatically reduces the CPU time of calculations. Comparison with the experimental and numerical data shows a good agreement between both of these data and the present results.

**Practical implications** – This method is an excellent tool for parametric study and preliminary design of hypersonic vehicles.

**Originality/value** – This method can predict convective heat flux in the leeward region where other similar methods are not applicable. In addition to this the present method is faster than other methods of solution for the 3D VSL equations.

**Keywords** Viscosity, Heat transfer, Approximation theory

**Paper type** Research paper

## Nomenclature

| | | | |
|---|---|---|---|
| $e_{\bar{\xi}}, e_{\bar{\beta}}, e_{\bar{n}}$ | = unit vectors of streamline curvilinear coordinate system | $\bar{\Gamma}, \bar{\delta}_{\varphi}$ | = body angles |
| $h_{\bar{\xi}}, h_{\bar{\beta}}$ | = scale factors of streamline coordinate system | $R_{\mathrm{N}}$ | = nose radius |
| $k_{\bar{\xi}}, k_{\bar{\beta}}$ | = streamline curvatures | $u, v, w$ | = velocity components |
| $\bar{\theta}$ | = streamline orientation | $q$ | = heat transfer rate |
| $Pr$ | = Prandtl number | $e_{\bar{s}}, e_{\bar{t}}$ | = tangential unit vectors on body surface |
| $P$ | = pressure | $\varepsilon$ | = Reynolds parameter, $\varepsilon = \sqrt{\mu_{\mathrm{ref}}/(\rho_{\infty} u_{\infty} R_{\mathrm{N}})}$ |
| $n_{\mathrm{b}}$ | = shock standoff distance | $\varepsilon^{+}$ | = ratio of eddy viscosity to dynamic viscosity, $\mu_t/\mu$ |
| $T$ | = temperature | | |

International Journal of Numerical Methods for Heat & Fluid Flow
Vol. 18 No. 1, 2008
pp. 36-49

0961-5539
DOI 10.1108/09615530810839732

$e_x, e_r, e_\varphi$ = unit vectors of cylindrical coordinate system
$\tilde{\xi}, \tilde{\beta}, \eta_n$ = computational coordinate system
$\rho$ = density
$\mu$ = viscosity
$x, r, \varphi$ = cylindrical coordinate system
$\alpha$ = angle of attack

*Subscripts*
$\infty$ = freestream condition
N = nose
ref = reference quantities
w = wall
b = body

## 1. Introduction

Aerodynamic heating is the most important parameter for the design of hypersonic vehicles, since it is a function of speed cubed. For the calculation of aerodynamic heating, the surface convective heat transfer coefficient must be determined. Such results may be obtained through the numerical solution of the Navier-Stokes (NS) equations (Gnoffo, 1990; Miyaji and Fujii, 1999) or one of their various subsets such as the Parabolized Navier-Stokes (PNS) equations (Helliwell *et al.*, 1981; Bhutta and Lewis, 1991) or viscous shock layer (VSL) equations (Maslov *et al.*, 1999; Gupta *et al.*, 1994, 1990).

Considerable attentions have been paid to the VSL equations since their solution needs less CPU times in comparison with the solution of NS and PNS equations (Anderson and Moss, 1975; Srivastava *et al.*, 1977). Moreover, VSL equations can be applied to both subsonic and supersonic regions. However, since the solution of three-dimensional VSL equations requires large computer storage and CPU time, this approach is not appropriate for a preliminary design where several geometries and flight trajectories are considered. To resolve this difficulty, approximate solution of VSL equations are proposed.

Grantz *et al.* (1990) added boundary-layer-like viscous terms to the inviscid streamwise momentum and energy equations, written in the shock coordinate system, to obtain a parabolic set of equations similar to the full axisymmetric VSL equations. They employed the second-order Maslen (1964) pressure relation instead of normal momentum equation, and employed a simple linear relation to express the component of velocity normal to the surface. Since, the shock shape was a part of the solution, no initial shock shape was necessary. This approximate axisymmetric VSL method of Grantz *et al.* had three disadvantages:

(1) too many iterations were required for shock shape convergence;

(2) the solution was inconsistent near the stagnation line; and

(3) the choice of node spacing across the shock layer was the cause of oscillations in the profiles of shock layer properties.

Cheatwood and DeJarnette (1994) developed another approximate axisymmetric VSL method. They started with the full axisymmetric VSL equations in a shock coordinate system. In these equations, they replaced the normal momentum equation by Maslen's second-order relation to calculate the pressure. The normal component of velocity, however, was calculated from the solution of continuity equation. In this method, shock shape is also determined as a part of the solution in both regions of subsonic and supersonic. The above-mentioned disadvantages of Grantz's method were resolved by this method of Cheatwood and DeJarnette. In addition, the method of Grantz *et al.* was not able to reduce the CPU time of calculation as compared with the solution of full VSL equations (Cheatwood and DeJarnette, 1994).

Malekzadeh Dirin *et al.* (2003) starting by writing the full three-dimensional VSL equations in a shock-oriented curvilinear coordinate system. In these equations, they replaced the normal momentum equation with the modified form of the Maslen's second-order pressure relation. They also solved the continuity equation to calculate the normal component of velocity. It is noted that in this work Malekzadeh Dirin *et al.* (2003) solved the three-dimensional VSL equations, in which, the shock shape was determined using the algorithm of Riley and DeJarnette (1992). As claimed by them, this method is three to five times faster than the original 3DVSL methods.

In all of the approximate methods, flow properties and aerodynamic heating are calculated only in the windward region. So the need for a fast method to calculate aerodynamic heating in the leeward region has been left unaddressed. To address this need, we applied axisymmetric analog (Cook, 1961) to the three-dimensional VSL equations, written in the streamline coordinate system. With this approximation the solution for circumferential velocity component, $w$, is not required anymore since it is set equal to zero. Maslen's second-order pressure relation is still solved instead of normal momentum equation, and continuity equation is solved to obtain normal component of velocity, $v$. With the use of streamline coordinate system, the calculation of aerodynamic heating in the leeward region becomes possible. Such an idea was used earlier by Kim *et al.* (1982) for the solution of the PNS equations. It is noted that the shock shape and the streamline orientations, which are required in the present method, are obtained using the algorithm of Riley and DeJarnette (1992). The orientations of streamlines in the leeward region, however, are calculated using the method of Karimian *et al.* (2003). The required CPU time of the present method for the solution of 3D VSL equations is less than that of Malekzadeh Dirin *et al.* (2003). Based on these achievements, the present method would be very attractive for the preliminary design studies of hypersonic vehicles.

## 2. Analysis

For the first time, Cook (1961) applied axisymmetric analog for the solution of three-dimensional boundary layer equations. This idea simplifies the equations and reduces the solution time dramatically by increasing the rate of convergence. Since, VSL equations are similar to the boundary layer equations, it is possible to apply the axisymmetric analog to the VSL equations. This is done through:

- derivation of the 3D VSL equations in the streamline curvilinear coordinate system; and
- applying axisymmetric analog along the streamlines in these equations.

As a result an axisymmetric form of VSL equations, valid along the streamlines, is obtained which dose not contain the crossflow velocity component, $w$.

Before the derivation of the above-mentioned axisymmetric form of VSL equations, we first present a description of streamline curvilinear coordinate system, and the method of determining surface-streamline orientations. Note that all of the variables used in this analysis are nondimensionlized by the reference quantities, presented in Appendix 1.

### *2.1 Coordinate system and streamline orientations*

The streamline curvilinear coordinate system $(\bar{\xi}, \bar{\beta}, \bar{n})$ is shown in Figure 1. $\bar{\xi}$ and $\bar{\beta}$ represent coordinates of a point on the body surface and $\bar{n}$ is the distance normal to the body. The unit vectors of this coordinate system is defined as, $e_{\bar{\xi}}$ which

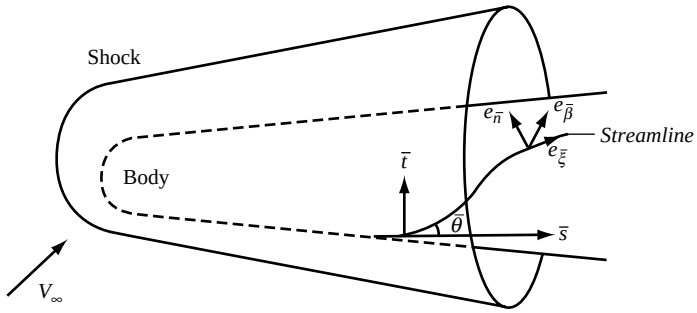


**Figure 1.**
Streamline curvilinear coordinate system

is in the streamline direction and tangent to the body, $e_{\bar{\beta}}$ that is perpendicular to $e_{\bar{\xi}}$ and tangent to the surface, and $e_{\bar{n}}$ which is perpendicular to $e_{\bar{\xi}}, e_{\bar{\beta}}$.

The surface of body is defined in the cylindrical coordinate system by $r_b = \bar{f}(x, \varphi)$. Unit vectors of streamline curvilinear coordinate system, now can be defined in terms of $e_x, e_r, e_\varphi$, as:

$$\begin{aligned} e_{\bar{\xi}} &= \cos\bar{\theta}\cdot e_{\bar{s}} + \sin\bar{\theta}\cdot e_{\bar{t}} \\ e_{\bar{\beta}} &= -\sin\bar{\theta}\cdot e_{\bar{s}} + \cos\bar{\theta}\cdot e_{\bar{t}} \\ e_{\bar{n}} &= -\sin\bar{\Gamma}\cdot e_x + \cos\bar{\Gamma}\cos\bar{\delta}_\varphi\cdot e_r - \cos\bar{\Gamma}\sin\bar{\delta}_\varphi\cdot e_\varphi \end{aligned} \tag{1}$$

where the tangential unit vectors on body surface $(e_{\bar{s}}, e_{\bar{t}})$ are defined as:

$$\begin{aligned} e_{\bar{s}} &= \cos\bar{\Gamma}\cdot e_x + \sin\bar{\Gamma}\cos\bar{\delta}_\varphi\cdot e_r - \sin\bar{\Gamma}\sin\bar{\delta}_\varphi\cdot e_\varphi \\ e_{\bar{t}} &= \sin\bar{\delta}_\varphi\cdot e_r + \cos\bar{\delta}_\varphi\cdot e_\varphi \end{aligned} \tag{2}$$

and the body angles $\bar{\Gamma}(x, \varphi)$ and $\bar{\delta}_\varphi(x, \varphi)$ are defined as:

$$\tan\bar{\Gamma} = \frac{\partial\bar{f}}{\partial x}\cos\bar{\delta}_\varphi, \quad \tan\bar{\delta}_\varphi = \frac{1}{\bar{f}}\frac{\partial\bar{f}}{\partial\varphi} \tag{3}$$

In equation (1), $\bar{\theta}$ denotes the angle between the streamlines and $e_{\bar{s}}$. Therefore, if $\bar{\theta}$ is determined on the body surface in windward and leeward regions, the streamline orientation would be determined on the surface.

The orientation of streamlines on the body surface in the windward region is found by applying momentum equations along the body surface in conjunction with the pressure distribution obtained from the inviscid solution (Riley and DeJarnette, 1992; Karimian and Malekzadeh Dirin, 2001). Consequently, the following expression is obtained:

$$\frac{1}{h_{\bar{\xi}}}\frac{\partial\bar{\theta}}{\partial\bar{\xi}} = -\frac{\sin\bar{\Gamma}}{h_{\bar{\xi}}}\frac{\partial\bar{\sigma}}{\partial\bar{\xi}} - \frac{1}{\rho_b\bar{u}_b^2}\frac{1}{h_{\bar{\beta}}}\frac{\partial P_b}{\partial\bar{\beta}} \tag{4}$$

where $\bar{\sigma} = \varphi - \bar{\delta}_\varphi$. The scale factor $h_{\bar{\beta}}$ is determined using the method of Karimian and Malekzadeh Dirin (2001).

In the leeward region, however, a linear interpolation which is based on the actual physical pattern of the flow in this region (Karimian *et al.*, 2003), is used to determine the streamline orientation as:

$$\bar{\theta} = 2\bar{\theta}_{\pi/2}\left(-\frac{1}{\pi}\,\varphi_{\mathrm{b}} + 1\right) \quad \frac{\pi}{2} \le \varphi_{\mathrm{b}} \le \pi \tag{5}$$

Now, with the determination of streamlines orientation, governing equations can be written along the streamline.

*2.2 Governing equations*

The 3DVSL equations for laminar, perfect gas flow were developed by Murray and Lewis (1978) in a body-oriented coordinate system. These equations were presented in a shock-oriented coordinate system by Malekzadeh Dirin *et al.* (2003).

In this paper, 3D VSL equations for laminar and turbulent flows are written in the streamline curvilinear coordinate system of $(\bar{\xi}, \bar{\beta}, \bar{n})$. For the sake of simplicity, the governing equations are transferred to the computational space of $(\tilde{\xi}, \tilde{\beta}, \eta_n)$, where:

$$\tilde{\xi} = \bar{\xi}, \quad \tilde{\beta} = \bar{\beta}, \quad \eta_n = 1 + \frac{\bar{n}}{n_{\mathrm{b}}} \tag{6}$$

and are presented in the form of:

$$A_0 \frac{\partial^2 W}{\partial \eta_n^2} + A_1 \frac{\partial W}{\partial \eta_n} + A_2 W + A_3 + A_4 \frac{\partial W}{\partial \tilde{\xi}} + A_5 \frac{\partial W}{\partial \tilde{\beta}} = 0 \tag{7}$$

In the above equation, $W$ represents the dependent variables $u$, $w$ and $h$ for $\tilde{\xi}$ momentum, $\tilde{\beta}$ momentum and energy equations, respectively. The nonlinear coefficients $A_0$, $A_1$, $A_2$, $A_3$, $A_4$ and $A_5$, are presented in Appendix 2.

The continuity equation is written in the form of:

$$\begin{aligned} &M \frac{\partial}{\partial \tilde{\xi}}(\rho u \bar{h}_3) + (\mathrm{MD} + \mathrm{NF}) \frac{\partial}{\partial \eta_n}(\rho u \bar{h}_3) + N \frac{\partial}{\partial \tilde{\beta}}(\rho u \bar{h}_3) - A \frac{\partial}{\partial \eta_n}(\rho v \bar{h}_1 \bar{h}_3) \\ &\quad + G \frac{\partial}{\partial \tilde{\xi}}(\rho w \bar{h}_1) + (\mathrm{GD} + \mathrm{KF}) \frac{\partial}{\partial \eta_n}(\rho w \bar{h}_1) + K \frac{\partial}{\partial \tilde{\beta}}(\rho w \bar{h}_1) = 0 \end{aligned} \tag{8}$$

where:

$$\begin{aligned} \bar{h}_1 &= h_{\bar{\xi}}(1 + \bar{n} k_{\bar{\xi}}) \\ \bar{h}_3 &= h_{\bar{\beta}}(1 + \bar{n} k_{\bar{\beta}}) \end{aligned} \tag{9}$$

and streamline curvatures are defined as:

$$k_{\bar{\xi}} = -\frac{1}{h_{\bar{\xi}}} \frac{\partial \bar{\Gamma}}{\partial \bar{\xi}}, \quad k_{\bar{\beta}} = -\frac{\cos \bar{\Gamma}}{h_{\bar{\beta}}} \frac{\partial \bar{\Gamma}}{\partial \bar{\beta}} \tag{10}$$

In the above relations the coefficients of $A$, $D$ and $F$ are defined as:

$$A = -\frac{1}{n_{\mathrm{b}}}, \quad D = -\frac{(\eta_n - 1)}{n_{\mathrm{b}}} \frac{\mathrm{d}n_{\mathrm{b}}}{\mathrm{d}\bar{\xi}}, \quad F = -\frac{(\eta_n - 1)}{n_{\mathrm{b}}} \frac{\mathrm{d}n_{\mathrm{b}}}{\mathrm{d}\bar{\beta}} \tag{11}$$

The values of $M$, $N$, $G$ and $K$ are functions of streamline curvatures, the distance between body and shock, body angles and shock angles.

At this stage, where the governing equations are obtained in the streamlines curvilinear coordinate, $w$ is set equal to zero, in order to implement the idea of axisymmetric analog.

## 3. Method of solution

The governing equations that will be solved in this paper are the equations obtained in Section 2.2 in which $w$ is set equal to zero. The shock shape which should be known before the solution of governing equations, is determined using the inviscid method of Riley and DeJarnette (1992). At each $\tilde{\xi}$, the governing equations are solved along the $\eta_n$ lines between the shock wave and the body; see Figure 2. At the shock wave, which is the outer boundary of the solution domain, the Rankine-Hugoniot relations are used to calculate the flow conditions at this boundary. At the surface of the body, no-slip boundary condition is applied and temperature is set equal to a fixed value.

Starting from the stagnation region, the first $\eta_n$ line would be the stagnation line. The governing equations along the stagnation line would be the limiting form of these equations which are obtained assuming $\tilde{\xi} \rightarrow 0$ (Malekzadeh Dirin *et al.*, 2002). For the rest of the domain, the solution is marched along the $\tilde{\xi}$ coordinate. At each $\tilde{\xi}$ Maslen's (1964) pressure relation, streamwise momentum equation and energy equation are solved, along the $\eta_n$ lines distributed in $\tilde{\beta}$ direction around the body, to obtain pressure, tangential velocity, and enthalpy, respectively. Density is, then, calculated from the equation of state.

Finally, the normal velocity is obtained through the solution of the continuity equation. The derivatives of $\tilde{\xi}, \tilde{\beta}$ in the governing equations are discretized using two-point backward difference scheme. The difference scheme used for the derivatives of $\eta_n$ is the second order and central. The final forms of discretized equations are solved using Thomas algorithm.

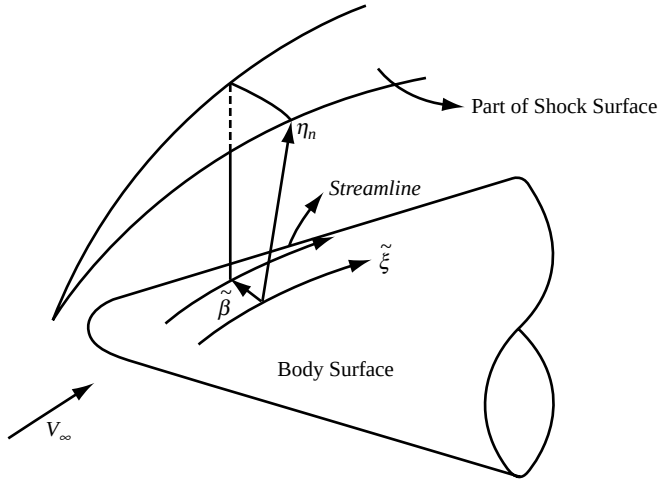


**Figure 2.**
Computational space between shock and body

In this paper, the Cebeci-Smith eddy-viscosity turbulence modeling (Cebeci and Smith, 1974) is employed in the system of equations. Cebeci-Smith model is a two-layer eddy-viscosity formulation whose inner layer value is based on Prandtl's mixing length concept and outer layer value is presented by Clauser-Klebanoff expression.

As mentioned at the end of Section 1 (i.e. Introduction), the shock shape and streamline orientations are obtained from the algorithm of Riley and DeJarnette (1992). Since, we were able to use this algorithm for axisymmetric bodies, the application of the present method has been demonstrated for three-dimensional flows around axisymmetric bodies. Note that the algorithm of Riley and DeJarnette (1992) is limited to blunt cone bodies.

## 4. Results

In an effort to evaluate the accuracy of this new method, several test cases are considered. Comparisons are made between the results of the present method, and the results of the existing numerical methods and experimental data (Cleary, 1969).

Surface heating rates of a 15° half angle blunted sphere-cone at various angles of attack are calculated. The results include heating rates of both laminar and turbulent flows of perfect gas in the windward and leeward regions. Two spherical nose radii of 0.00952 and 0.0279 m are considered. The freestream conditions are $\rho_\infty = 0.00973\,\mathrm{kg/m^3}$, $T_\infty = 47.3°\mathrm{K}$ and $M_\infty = 10.6$ with a wall temperature of $T_w = 300°\mathrm{K}$. In the $\tilde{\xi}$ direction, the step size of 0.1 of $R_N$ is used. In $\eta_n$ direction, the nodes are made dense near the body. Our experience shows that 51 nodes in $\eta_n$ direction are enough to obtain accurate results for laminar flow. For the $\tilde{\beta}$ direction, $\Delta\tilde{\beta}$ is 5°, i.e. 19 nodes are chosen for the half of the solution domain. The above mentioned grid spacing is determined through the grid convergence study. This grid convergence study is for both laminar and turbulent flows. As will be seen, $\eta_n$ larger than 51 does not change the results in laminar part. Similarly, $\Delta\tilde{\xi} \leq 0.1R_N$ and $\Delta\tilde{\beta} \leq 5°$ will not change the results in laminar flow.

In Figure 3, the heating rates of laminar perfect gas flow around a 15° sphere cone with $R_N = 0.00952\,\mathrm{m}$ at 5 and 10° angles of attack are shown on the windward plane. As is shown, results of present work are in good agreement with experimental data. In comparison to the method of Malekzadeh Dirin *et al.* (2003), 33 percent reduction in

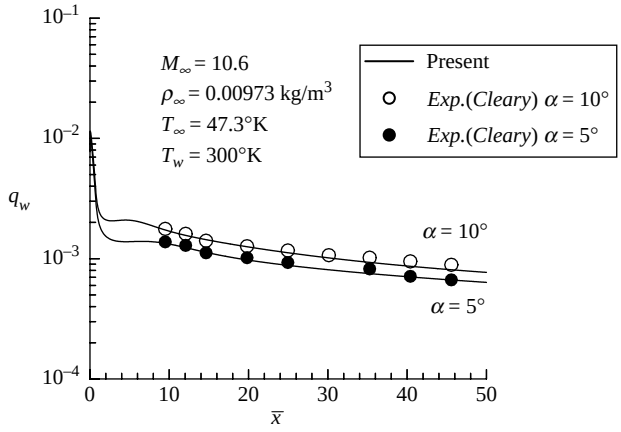


**Figure 3.**
Heat transfer comparison in windward plane, $R_N = 0.00952\,\mathrm{m}$

CPU time is observed, which is very important for preliminary design. A detailed CPU time comparison will be presented later in Table I.

The heating rates calculated by the present method in the leeward plane of a sphere cone with $R_N = 0.0279$ m at 5 and 10° angles of attack are shown in Figure 4. As is seen, present results have excellently predicted the $q_w$, obtained from experiments of Cleary (1969). The small difference between the present results and the experimental data is due to the thick shock layer which occurs in the leeward region. It is noted that Maslen's relation would not be an appropriate assumption for a very thick shock layer.

Circumferential heat transfer results for laminar flow around a blunted cone of $R_N = 0.0279$ m at 5 and 10° angles of attack are shown in Figures 5 and 6 for two axial locations of $\bar{x} = 4.86$ and $\bar{x} = 15.4$. As is seen, the accuracy of present results in both windward and leeward regions is evident when compared with the experimental data. This demonstrates the capability of the present approximate 3D VSL solver for prediction of heat transfer rates even in the leeward region.

A CPU time comparison between the results of present method and those of Malekzadeh Dirin *et al.* (2003) is presented here. The computer used for this study includes a Pentium IV processor, and Ram of 512 Meg. The flowfiled and the sphere cone are the same as the one in Figure 3, however, the solution is marched only up to 10 $R_N$ for this CPU time comparison. The results are shown in Table I. As was mentioned earlier a 33 percent reduction in CPU time is obtained. This time reduction is important for preliminary design, where consideration of several geometries and flight path is necessary.

| | Present method | Method of Malekzadeh Dirin *et al.* (2003) |
|---|---|---|
| CPU time (s) | 40 | 60 |
| $\Delta\tilde{\xi}/R_N$ | 0.1 | 0.1 |
| No. of nodes in $\eta_n$ | 51 | 51 |
| No. of nodes in $\tilde{\beta}$ | 19 | 19 |

**Notes:** 15° sphere cone; $R_N = 0.00952$ m; $\alpha = 10°$ for length of 10 $R_N$

**Table I.**
CPU time comparison

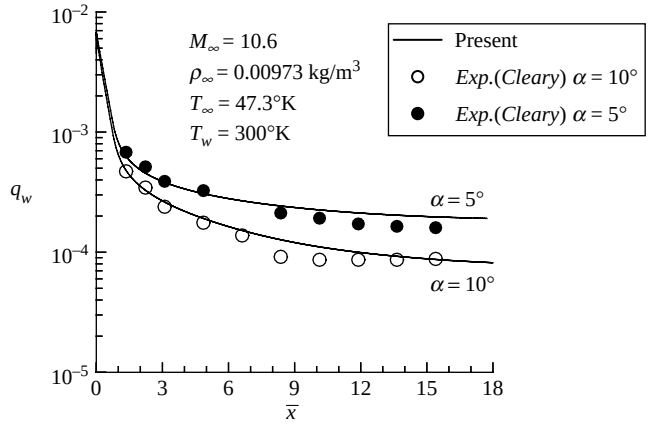


**Figure 4.**
Heat transfer comparison in leeward plane, $R_N = 0.0279$ m

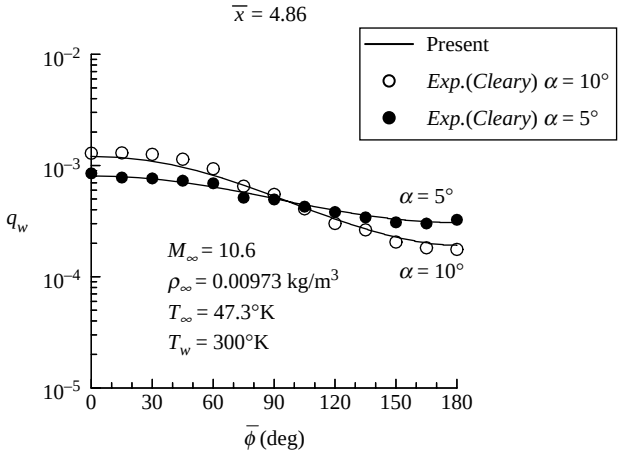


**Figure 5.**
Circumferential heat transfer comparison, $R_N = 0.0279$ m

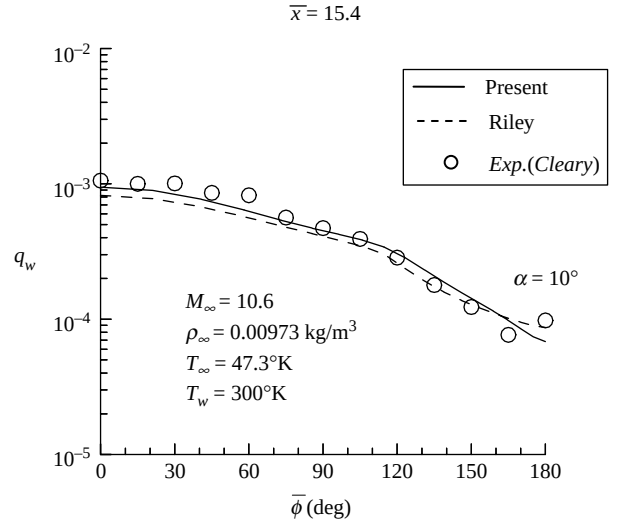


**Figure 6.**
Circumferential heat transfer comparison, $R_N = 0.0279$ m

For turbulent flow comparison, the results of the present method are compared with those of Malekzadeh Dirin *et al.* (2003). Since, both are numerical results, the credibility of them are considered first by a grid convergence study. Although the results of this study, shown in Figures 7 and 8, are from the present method, the same trend is observed for the results of Malekzadeh Dirin *et al.* (2003). According to Table II, for $\Delta\tilde{\xi} = 0.03R_N$ and 19 nodes in $\tilde{\beta}$ direction, the effect of various nodes in $\eta_n$ direction is given through cases a.1-a.5. As seen in Figure 7, there is no changes between a.4 and a.5 curves. Therefore, 151 nodes in $\eta_n$ direction is enough. Cases b1-b.3 demonstrate the effect of different $\Delta\tilde{\xi}$ values for fixed node numbers of 151 and 19 in directions $\eta_n$ and $\tilde{\beta}$, respectively. As is seen in Figure 8, there is no different between these results.

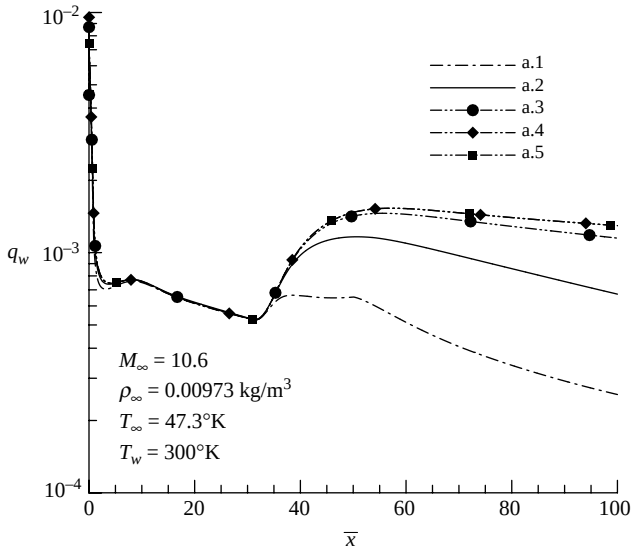


**Figure 7.**
Effect of number of nodes in $\eta_n$ direction on the surface heat transfer distribution, $R_N = 0.0279$ m

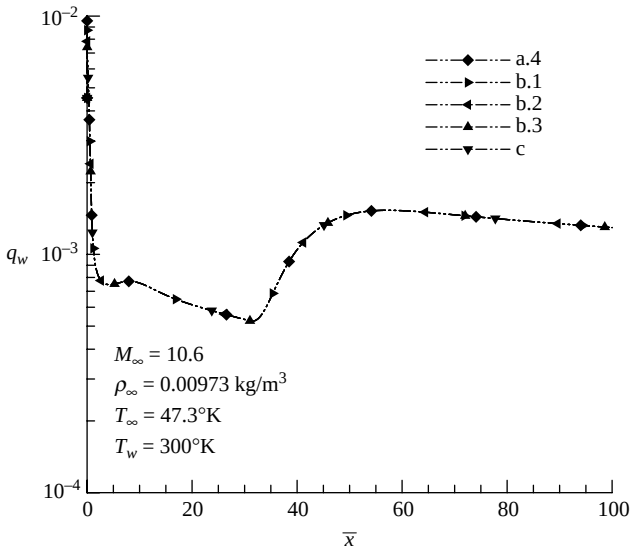


**Figure 8.**
Effect of $\Delta\tilde{\xi}$ and $\Delta\tilde{\beta}$ on the surface heat transfer distribution, $R_N = 0.0279$ m

Therefore, a value of $\Delta\tilde{\xi} = 0.1R_N$ is appropriate. The effect of different node numbers in $\tilde{\beta}$ direction can be seen by comparing results of cases a.4 and c in Figure 8. Again as seen no difference is observed between these results. Therefore, 19 node numbers in $\tilde{\beta}$ direction is enough.

Now we compare the results of the present method with the results of Malekzadeh Dirin *et al.* (2003) for $\Delta\tilde{\xi} = 0.1R_N$, 151 nodes in $\eta_n$ direction, and 19 nodes in $\tilde{\beta}$ direction

| Cases | $\Delta\tilde{\xi}/R_N$ | No. of nodes in $\eta_n$ direction | No. of nodes in $\tilde{\beta}$ direction |
|---|---|---|---|
| a.1 | 0.03 | 25 | 19 |
| a.2 | 0.03 | 51 | 19 |
| a.3 | 0.03 | 101 | 19 |
| a.4 | 0.03 | 151 | 19 |
| a.5 | 0.03 | 201 | 19 |
| b.1 | 0.015 | 151 | 19 |
| b.2 | 0.06 | 151 | 19 |
| b.3 | 0.1 | 151 | 19 |
| c | 0.1 | 151 | 29 |

**Table II.**
Grid specifications for turbulent cases

in Figure 9. The excellent match of both results in turbulent region is clear. Note that both results are obtained for a fixed transition point of $\bar{x} = 30$.

At the end, we conclude that the present 3D VSL approximate method provides a computational capability which reduces the CPU time, and expands the range of application for the prediction of hypersonic heating rates.

## 5. Conclusions

An approximate axisymmetric method has been developed to calculate three-dimensional viscous hypersonic flows. In this method, 3D VSL equations are reduced to an axisymmetric form by using the axisymmetric analog. Normal momentum equation is still substituted by Maslen equation. Governing equations are solved in a streamline curvilinear coordinate system to predict surface heating rates in both windward and leeward regions. With the present method the surface heating rates were predicted very well when comparing with experimental data. This was achieved with a 33 percent reduction in CPU time when compared to Malekzadeh Dirin *et al.* (2003).

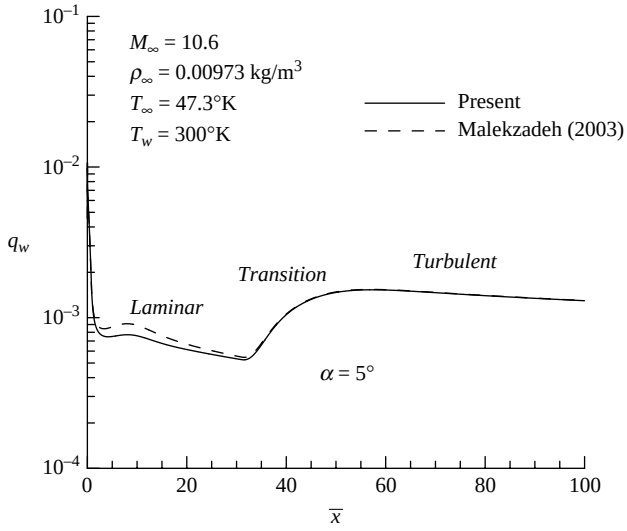


**Figure 9.**
Heat transfer comparison in windward plane, $R_N = 0.0279$ m

In addition calculation of heating rates at the leeward region was also become possible with the present method.

## References

Anderson, E.C. and Moss, J.N. (1975), "Numerical solution of the hypersonic viscous-shock layer equations for laminar-transitional and turbulent flows of a perfect gas over blunt axially symmetric bodies", NASA TN- D-7865.

Bhutta, B.A. and Lewis, C.H. (1991), "Comparison of hypersonic experiments and PNS predictions, Part I: aerothermodynamics", *Journal of Spacecraft*, Vol. 28 No. 4, pp. 376-86.

Cebeci, T. and Smith, A.M.O. (1974), *Analysis of Turbulent Boundary Layers*, Academic Press, New York, NY, pp. 215-17, 256, 264.

Cheatwood, F.M. and DeJamentte, F.R. (1994), "Approximate viscous shock-layer technique for calculating hypersonic flows about blunt. Nosed bodies", *Journal of Spacecraft and Rockets*, Vol. 31 No. 4, pp. 621-8.

Cleary, J.W. (1969), "Effects of angle of attack and bluntness on laminar heating rate distribution on a 15 degree cone at a Mach number of 10.6", NASA TN5450.

Cook, J.C. (1961), "An axially symmetric analogue for general three-dimensional boundary layer", British A.R.C., R & M, No. 3200.

Gnoffo, P.A. (1990), "An upwind-biased point implicit relaxation algorithm for viscous, compressible perfect-gas flows", NASA TP 2953.

Grantz, A.C., DeJarnette, F.R. and Thompson, R.A. (1990), "Approximate viscous-shock layer method for hypersonic flows over blunt-nosed bodies", *Journal of Spacecraft and Rockets*, Vol. 27 No. 6, pp. 597-605.

Gupta, R.N., Zoby, E.V., Nayani, S.N. and Lee, K.P. (1994), "High-order viscous shock-layer solutions for high-altitude flows", *Journal of Spacecraft and Rockets*, Vol. 31 No. 5, pp. 751-8.

Gupta, R.N., Lee, K.P., Zoby, E.V., Moss, J.N. and Thompson, R.A. (1990), "Hypersonic viscous shock-layer solutions over long slender bodies – Part I: high Reynolds number flows", *Journal of Spacecraft*, Vol. 27 No. 2.

Helliwell, W.S., Dickson, R.P. and Lubard, S.C. (1981), "Viscous flow over arbitrary geometries at high angles of attack", *AIAA Journal*, Vol. 19 No. 2, pp. 191-7.

Karimian, S.M.H. and Malekzadeh Dirin, M. (2001), "Approximate solution of inviscid flow around the nose of hypersonic bodies at angle of attack", *Amirkabir Journal*, Vol. 12 No. 47.

Karimian, S.M.H., Malekzadeh Dirin, M. and Maerefat, M. (2003), "An engineering inviscid-boundary layer method for calculation of aerodynamic heating in the leeward region", paper presented at 41st CFD Conference.

Kim, M.D., Thareja, R.R. and Lewis, C.H. (1982), "Three-dimensional viscous flowfield computations in a streamline coordinate system", *Journal of Spacecraft*, Vol. 19 No. 1.

Malekzadeh Dirin, M. (2002), "Development of an approximate-engineering method for calculating of aerodynamic heating and flow analysis in the leeward region of hypersonic three-dimensional bodies", PhD thesis, Department of Mechanical Engineering, Faculty of Engineering, Tarbiat-Modares University, Tehran.

Malekzadeh Dirin, M., Marefat, M. and Karimian, S.M.H. (2003), "Approximate three-dimensional viscous shock-layer method for hypersonic flow over blunt-nosed bodies", AIAA Paper 03-154.

Maslen, S.H. (1964), "Inviscid hypersonic flow past smooth symmetric bodies", *AIAA Journal*, Vol. 2, pp. 1055-61.

Maslov, A.A., Mironov, S.G., Poplavskaya, T.V., Shiplyuk, A.N. and Vetlutsky, V.N. (1999), "Viscous shock layer on a plate in hypersonic flow", *Eur. J. Mech. B/Fluids*, Vol. 18 No. 2.

Miyaji, K. and Fujii, K. (1999), "Numerical analysis of three-dimensional shock/shock interactions and the aerodynamic heating", AIAA-99-0144.

Murray, A.L. and Lewis, C.H. (1978), "Hypersonic three-dimensional viscous shock layer flows over blunt bodies", *AIAA Journal*, Vol. 16 No. 12, pp. 1279-86.

Riley, C.J. and DeJarnette, F.R. (1992), "Engineering aerodynamic heating method for hypersonic flow", *Journal of Spacecraft and Rockets*, Vol. 29 No. 3.

Srivastava, B.N., Werle, M.J. and Davis, R.T. (1977), "Viscous shock-layer solutions for hypersonic sphere-cones", AIAA Paper, 77-693.

## Appendix 1

In this paper, all variables are nondimensionlized by the following relation:

$$x=\frac{x'}{R_{\mathrm{N}}},\quad V=\frac{V'}{V'_{\infty}},\quad \rho=\frac{\rho'}{\rho'_{\infty}},\quad \rho=\frac{\rho'}{\rho'_{\infty}V'^{2}_{\infty}},\quad h=\frac{h'}{V'^{2}_{\infty}},\quad T=\frac{T'}{T'_{\infty}},\quad \mu=\frac{\mu'}{\rho'_{\infty}V'_{\infty}R_{\mathrm{N}}},\quad q=\frac{q'}{\rho'_{\infty}V'^{3}_{\infty}}$$

## Appendix 2

Momentum and energy equations may be written in the form of:

$$A_0\frac{\partial^2 W}{\partial \eta_n^2}+A_1\frac{\partial W}{\partial \eta_n}+A_2W+A_3+A_4\frac{\partial W}{\partial \tilde{\xi}}+A_5\frac{\partial W}{\partial \tilde{\beta}}=0$$

where $W$ represents the dependent variables $u$, $w$ and $h$ for $\tilde{\xi}$ momentum, $\tilde{\beta}$ momentum and energy equations, respectively. The nonlinear coefficients $A_0$, $A_1$, $A_2$, $A_3$, $A_4$ and $A_5$ are:
$\tilde{\xi}$ *momentum*:

$$A_0=-\frac{\varepsilon^2}{\rho}\mu A^2(1+\varepsilon^+)$$

$$A_1=-vA-\frac{\varepsilon^2}{\rho}A^2\frac{\partial \mu}{\partial \eta_n}(1+\varepsilon^+)-\frac{\varepsilon^2}{\rho}\mu A^2\frac{1}{\bar{h}_1}\frac{\partial \bar{h}_1}{\partial \eta_n}$$
$$+\frac{\varepsilon^2}{\rho}\mu A^2\left(\frac{2}{\bar{h}_1}\frac{\partial \bar{h}_1}{\partial \eta_n}+\frac{1}{\bar{h}_3}\frac{\partial \bar{h}_3}{\partial \eta_n}\right)(1+\varepsilon^+)+(\mathrm{MD}+\mathrm{NF})\frac{u}{\bar{h}_1}+(\mathrm{GD}+\mathrm{KF})\frac{w}{\bar{h}_3}-\frac{\varepsilon^2}{\rho}\mu A^2\frac{\partial \varepsilon^+}{\partial \eta_n}$$

$$A_2=-vA\frac{1}{\bar{h}_1}\frac{\partial \bar{h}_1}{\partial \eta_n}+\frac{w}{\bar{h}_1\bar{h}_3}\left[G\frac{\partial \bar{h}_1}{\partial \tilde{\xi}}+(\mathrm{GD}+\mathrm{KF})\frac{\partial \bar{h}_1}{\partial \eta_n}+K\frac{\partial \bar{h}_1}{\partial \tilde{\beta}}\right]$$
$$+\frac{\varepsilon^2}{\rho}A^2\frac{\partial \mu}{\partial \eta_n}\frac{1}{\bar{h}_1}\frac{\partial \bar{h}_1}{\partial \eta_n}+\frac{\varepsilon^2}{\rho}\mu A^2\left(\frac{1}{\bar{h}_1}\frac{\partial \bar{h}_1}{\partial \eta_n}\right)\left(\frac{2}{\bar{h}_1}\frac{\partial \bar{h}_1}{\partial \eta_n}+\frac{1}{\bar{h}_3}\frac{\partial \bar{h}_3}{\partial \eta_n}\right)$$

$$A_3=-\frac{w^2}{\bar{h}_1\bar{h}_3}\left[M\frac{\partial \bar{h}_3}{\partial \tilde{\xi}}+(\mathrm{MD}+\mathrm{KF})\frac{\partial \bar{h}_3}{\partial \eta_n}+N\frac{\partial \bar{h}_3}{\partial \tilde{\beta}}\right]$$
$$+\frac{1}{\rho\bar{h}_1}\left[M\frac{\partial P}{\partial \tilde{\xi}}+(\mathrm{MD}+\mathrm{KF})\frac{\partial P}{\partial \eta_n}+N\frac{\partial P}{\partial \tilde{\beta}}\right]$$

$$A_4=\frac{u}{\bar{h}_1}M+\frac{w}{\bar{h}_3}G$$

$$A_5=\frac{u}{\bar{h}_1}N+\frac{w}{\bar{h}_3}K$$

$\bar{\beta}$ *momentum*:

$$A_0 = -\frac{\varepsilon^2}{\rho}\mu A^2$$

$$A_1 = -vA - \frac{\varepsilon^2}{\rho}A^2\frac{\partial\mu}{\partial\eta_n} - \frac{\varepsilon^2}{\rho}\mu A^2\left(\frac{1}{\bar{h}_1}\frac{\partial\bar{h}_1}{\partial\eta_n}+\frac{1}{\bar{h}_3}\frac{\partial\bar{h}_3}{\partial\eta_n}\right) + (\mathrm{MD}+\mathrm{NF})\frac{u}{\bar{h}_1} + (\mathrm{GD}+\mathrm{KF})\frac{w}{\bar{h}_3}$$

$$A_2 = -vA\frac{1}{\bar{h}_3}\frac{\partial\bar{h}_3}{\partial\eta_n} + \frac{u}{\bar{h}_1\bar{h}_3}\left[M\frac{\partial\bar{h}_3}{\partial\tilde{\xi}} + (\mathrm{MD}+\mathrm{KF})\frac{\partial\bar{h}_3}{\partial\eta_n} + N\frac{\partial\bar{h}_3}{\partial\tilde{\beta}}\right]$$
$$+\frac{\varepsilon^2}{\rho}A^2\frac{\partial\mu}{\partial\eta_n}\frac{1}{\bar{h}_3}\frac{\partial\bar{h}_3}{\partial\eta_n} + \frac{\varepsilon^2}{\rho}\mu A^2\frac{1}{\bar{h}_3}\left(\frac{\partial\bar{h}_3}{\partial\eta_n}\right)^2 + \frac{\varepsilon^2}{\rho}\mu A^2\frac{1}{\bar{h}_1\bar{h}_3}\frac{\partial\bar{h}_1}{\partial\eta_n}\frac{\partial\bar{h}_3}{\partial\eta_n}$$

$$A_3 = -\frac{u}{\bar{h}_1\bar{h}_3}\left[G\frac{\partial\bar{h}_1}{\partial\tilde{\xi}} + (\mathrm{GD}+\mathrm{KF})\frac{\partial\bar{h}_1}{\partial\eta_n} + K\frac{\partial\bar{h}_1}{\partial\tilde{\beta}}\right] + \frac{1}{\rho\bar{h}_3}\left[G\frac{\partial P}{\partial\tilde{\xi}} + (GD+KF)\frac{\partial P}{\partial\eta_n} + K\frac{\partial P}{\partial\tilde{\beta}}\right]$$

$$A_4 = \frac{u}{\bar{h}_1}M + \frac{w}{\bar{h}_3}G$$

$$A_5 = \frac{u}{\bar{h}_1}N + \frac{w}{\bar{h}_3}K$$

*Energy*:

$$A_0 = -\frac{\varepsilon^2}{\rho}\frac{\mu}{Pr}A^2\left(1+\varepsilon^+\frac{Pr}{Pr_t}\right)$$

$$A_1 = -vA - \frac{\varepsilon^2}{\rho}\frac{A^2}{Pr}\frac{\partial\mu}{\partial\eta_n}\left(1+\varepsilon^+\frac{Pr}{Pr_t}\right)$$
$$-\frac{\varepsilon^2}{\rho}\frac{\mu}{Pr_t}A^2\frac{\partial\varepsilon^+}{\partial\eta_n} - \frac{\varepsilon^2}{\rho}\frac{\mu}{Pr}\left(\frac{1}{\bar{h}_1}\frac{\partial\bar{h}_1}{\partial\eta_n}+\frac{1}{\bar{h}_3}\frac{\partial\bar{h}_3}{\partial\eta_n}\right)\left(1+\varepsilon^+\frac{Pr}{Pr_t}\right) + (\mathrm{MD}+\mathrm{NF})\frac{u}{\bar{h}_1} + (\mathrm{GD}+\mathrm{KF})\frac{w}{\bar{h}_3}$$

$$A_2 = 0$$

$$A_3 = \frac{vA}{\rho}\frac{\partial P}{\partial\eta_n} - \frac{u}{\rho\bar{h}_1}\left[M\frac{\partial P}{\partial\tilde{\xi}} + (\mathrm{MD}+\mathrm{KF})\frac{\partial P}{\partial\eta_n} + N\frac{\partial P}{\partial\tilde{\beta}}\right] - \frac{w}{\rho\bar{h}_3}\left[G\frac{\partial P}{\partial\tilde{\xi}} + (\mathrm{GD}+\mathrm{KF})\frac{\partial P}{\partial\eta_n} + K\frac{\partial P}{\partial\tilde{\beta}}\right]$$
$$-\frac{\varepsilon^2}{\rho}\mu\left(\frac{u}{\bar{h}_1}\frac{\partial\bar{h}_1}{\partial\eta_n}A\right)^2 - \frac{\varepsilon^2}{\rho}\mu(1+\varepsilon^+)\left[\left(A\frac{\partial u}{\partial\eta_n}\right)^2 - 2A^2\frac{u}{\bar{h}_1}\frac{\partial\bar{h}_1}{\partial\eta_n}\frac{\partial u}{\partial\eta_n}\right]$$

$$A_4 = \frac{u}{\bar{h}_1}M + \frac{w}{\bar{h}_3}G$$

$$A_5 = \frac{u}{\bar{h}_1}N + \frac{w}{\bar{h}_3}K$$

**Corresponding author**
S. Noori can be contacted at: s_noori@aut.ac.ir